

Transmembrane Protein Activation Refined by Site-Specific Hydration Dynamics**

Sunyia Hussain, John M. Franck, and Songi Han*

Transmembrane proteins are the gatekeepers of the cell—channels that allow ions and molecules to enter or exit, or receptors that respond to their surroundings to change conditions inside the cell. The conformational dynamics of membrane protein activation are key to understanding the details of their function,^[1–4] and yet such information has proven to be difficult to obtain because of the experimental challenges involved in obtaining dynamics information for large hydrophobic protein complexes. Various magnetic resonance techniques, including magic-angle-spinning solid-state NMR (ssNMR) spectroscopy,^[5] NMR relaxation measurements,^[6] and electron paramagnetic resonance (EPR) spectroscopy,^[1,3] are at the frontier for capturing elusive details of membrane protein structure and dynamics. Here, we demonstrate the use of a novel combination of methods to present a dynamics-based picture that relates the structure of a membrane protein segment to the functional movement it supports. This is achieved by observing the surrounding hydration water, which rearranges simultaneously with protein conformational changes incurred upon activation.

We obtained site-specific hydration dynamics information by using the NMR-signal-enhancement technique Over-


hauser dynamic nuclear polarization (ODNP), which was recently developed for probing local water diffusivity within approximately 10 Å (2–4 water layers) of a nitroxide radical spin-labeled amino acid residue.^[7–12] This technique, combined with EPR lineshape analysis, which captures protein segment mobility around the spin label, offers a snapshot of distinct dynamic changes experienced by the protein as well as the solvating water. In addition, a newly developed analysis allows the separation of two important modes of water dynamics detected by ODNP. This new method isolates the contribution of 1) freely translating “hydration water”, which experiences fast, picosecond scale, motion, from 2) nanosecond timescale fluctuations in the spin interactions due to “bound” water molecules with slower dynamics or labile amide protons.

In this study, ODNP is used to observe the photoactivation of a seven-helical transmembrane (7TM) proton pump, proteorhodopsin (PR). 7TMs form a broad class of proteins, including many physiologically relevant receptors and approximately 40% of drug targets.^[13] We clarify changes in protein site-specific water dynamics around a critical PR segment upon activation, both on the picosecond and nanosecond timescales. The quantitative description of hydration dynamics across a biological interface still remains a challenging objective. Current EPR-based techniques used to study water in membrane protein systems either require cryogenic temperatures^[14,15] or the introduction of a soluble chemical agent,^[16] whereas ODNP can directly evaluate water motion around the spin label under ambient conditions, as has recently been demonstrated for protein folding^[12] and the conformational change of a membrane transporter.^[17]

Hydration water has been hypothesized to be an important determinant for the function of globular proteins,^[18–20] but its role in the mechanics of transmembrane proteins is particularly complicated by the additional effect of the surrounding lipids, which have been thought to be the more influential solvent.^[21,22] However, recent experimental and theoretical work on bovine rhodopsin (Rh)^[23,24] and bacteriorhodopsin (BR)^[25,26] suggest that internal protein hydration does influence function and is indeed altered upon protein activation. Recent ssNMR work complements neutron-scattering studies of global hydration properties,^[26] by enabling site-specific resolution to probe the heterogeneous landscape of the protein–lipid–water assembly. These studies clearly demonstrate the link between surface hydration and function around the mobile loop residues^[27] and the transmembrane G helix of PR.^[28] However, ssNMR can only differentiate whether or not a residue is hydrated, whereas ODNP is uniquely capable of resolving finer variations in hydration water dynamics.

[*] S. Hussain, Dr. J. M. Franck, Prof. S. Han
Department of Chemical Engineering and Department of Chemistry
and Biochemistry, University of California, Santa Barbara
Santa Barbara, CA 93016 (USA)
E-mail: songi@chem.ucsb.edu

[**] This work was supported by the Institute for Collaborative Biotechnologies through grant W911NF-09-0001 from the U.S. Army Research Office. The content of the information does not necessarily reflect the position or the policy of the Government, and no official endorsement should be inferred. We also acknowledge support by the Packard foundation for Science and Engineering, and the use of NMR facilities funded by the NSF MRSEC grant DMR-1121053. J.M.F. acknowledges support of the Elings Postdoctoral Fellowship, UCSB CNSI. We thank Dr. Alexander Mikhailovsky for the setup and design of time-resolved optical absorption spectroscopy, Devin Edwards and Evan Geller for the setup of the laser-triggered EPR spectroscopy, and Dr. Katherine Stone, Anna Pavlova, Jeda Voska, Christopher Carnabatu, Aye Aye, and Maia Kinnebrew for development of molecular biology and protein purification procedures. The PR gene with the E108Q mutation and His-tag was provided by Dr. Gregg Whited (Genencor). Our work on PR started as a collaboration with Prof. Galen Stucky, Christopher Knoll, Dr. Chi Nguyen, Dr. Hongjun Liang, and Dr. Gregg Whited. We also thank Dr. Brandon Armstrong for apomyoglobin ODNP data given in the Supporting Information.

 Supporting information (containing experimental details, including spin-labeled protein sample preparation and methodology for EPR, ODNP, and optical absorption spectroscopy) for this article is available on the WWW under <http://dx.doi.org/10.1002/anie.201206147>.

The 10–15 Å range of sensitivity inherent to ODNP enables the resolution of diffusion dynamics within the local volume of water surrounding a small nitroxide spin probe attached to a protein site, spanning 2–4 water layers above the biological surface. The high polarization of the EPR transition is saturated by microwave irradiation, transferred to the nuclear spins as they diffuse through these few water layers near the spin label, and ultimately manifests as an enhancement of the water's proton NMR signal. The concentration-independent ODNP coupling factor ξ is extracted by measuring first the increase in signal enhancement with increasing microwave power (example data shown in the Supporting Information, Figure S1), and, second, the proton spin lattice relaxation times in both the absence and presence of a spin label. As the value of ξ depends on the fluctuating interactions between the spin label and the spins in the nearby, translationally mobile water molecules, it encodes information about the dynamics of the water molecules as they pass near the spin label. It is most convenient to convert ξ into a timescale (i.e. correlation time, τ) associated with the motion of hydration water.^[7,29] High values for ξ correspond to low τ and faster local water diffusion. For reference, the parameters for bulk water obtained from free nitroxide in solution are $\xi = 0.33$ and $\tau = 33$ ps.^[8,30] As the value of ξ contains contributions from both tens of MHz and tens of GHz fluctuations, one must be cautious when performing this conversion into τ .^[7,29]

The translational model^[29] for hydration dynamics has extensively been shown to reveal trends for local water diffusion in and around various biological surfaces and interfaces measured by ODNP^[11,12,31,32] by providing a direct conversion between ξ and τ .^[7] However, the heterogeneous protein environment—particularly the contribution of more-tightly bound slow water molecules—adds complexity to such an analysis. To account for this, the coupling factor can be broken down as a ratio of two relaxivities: $\xi = k_o/k_p$. The ODNP parameters k_o and k_p are transition rates with units $s^{-1}M^{-1}$; the cross-relaxivity k_o depends on fluctuations of the spin interactions at tens of GHz, and therefore exclusively reports on the fast, ps scale, free-water dynamics, whereas the self-relaxivity k_p additionally contains a contribution from fluctuations at the NMR frequency (15 MHz). The contribution from ps water dynamics can be subtracted from k_p to extract the relaxivity k_{low} , which depends exclusively on fluctuations at the 15 MHz frequency, and we present it here as an evaluator of ns scale bound hydration water. This strict separation of timescales is only feasible by using both NMR relaxation and ODNP measurements (see the Supporting Information for more details of theory and analysis).

ODNP analysis of the intracellular E–F loop of PR accurately maps the heterogeneity of the hydration water to the degree that an α -helical structural element is visible from the trend in water dynamics across the loop, as expressed by the general parameter ξ , the exclusively fast-motion component k_o (Figure 1a and b), and the variation in bound water molecules observed by k_{low} (Figure S2 in the Supporting Information). We chose to probe the dynamic properties of this loop segment of PR because studies of BR^[33–35] and Rh^[36] have revealed that this function-relevant region moves upon

photoactivation; this observation could explain the difficulty of obtaining crystal-structure coordinates for this segment.^[37–39] The residue-to-residue hydration dynamics reveal a periodic pattern with significant contrast, with the approximately 3.6 residue length of an α helix being clearly visible for PR in β -dodecylmaltoside (DDM) micelles (Figure 1a and b). The fast ps scale water dynamics therefore map a secondary structure element and give direct information about its placement with respect to the protein or detergent surface, where water motion would be hindered. We found that sites G171, K172, and C175 are buried ($\tau = 600$ –850 ps, $k_o/k_{o,bulk} < 0.4$), whereas sites S173, A174, N176, and T177 are exposed to

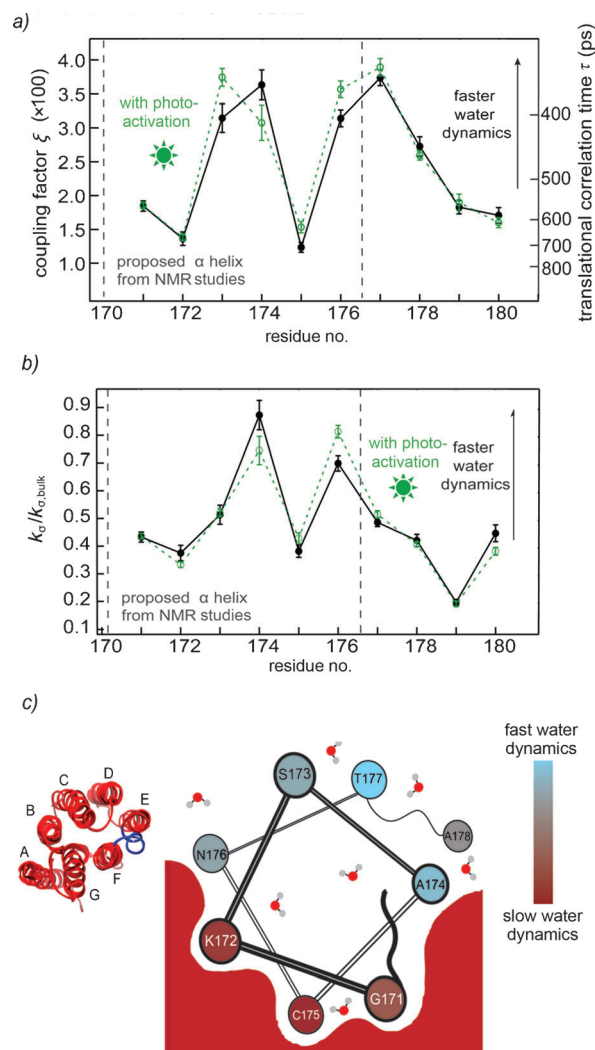


Figure 1. Evidence for the α -helical structure of the E–F loop of PR, with the proposed structure from recent NMR studies indicated.^[40,42] a) Hydration dynamics measured by ODNP, given by coupling factor, ξ , and the translational correlation time of water, τ , with measurements upon photoactivation given by the green trace. b) Extraction of fast (ps scale) translational water dynamics by k_o , normalized by $k_{o,bulk} = 116 s^{-1} M^{-1}$, the corresponding reference value from free nitroxide (4-hydroxy-TEMPO). c) The E–F loop structure represented by a helical wheel schematic summarizes the EPR and ODNP results (color shading is based on ξ). Spin-labeled protein concentrations are ca. 450 μM , and buffer conditions are 0.05 % DDM, 50 mM phosphate, 150 mM KCl, pH 9.5.

the aqueous solvent ($\tau = 400\text{--}450$ ps, $k_o/k_{o,\text{bulk}} > 0.5$). This topology for the E–F loop is also confirmed by the trend in k_{low} —a high degree of bound water molecules is evident for buried sites K172 and C175, whereas the solvent-exposed sites S173 and T177 experience the lowest contribution from tightly-associated water molecules (Figure S2 in the Supporting Information).

Information inferred from ODNP data regarding the contact of the E–F loop with the protein surface (Figure 1 c) is supplemented by a detailed site-specific EPR lineshape study of the same sites (Figure S3 in the Supporting Information). The measurements include: 1) central line broadening, which determines general backbone/side-chain stiffness, and 2) characteristic EPR spectral features for immobile/mobile components, which signify the presence of tertiary interactions of amino acid side chains with protein or surfactant surfaces (Figure S4 in the Supporting Information). This analysis reveals a consistent periodic trend in both the amino acid mobilities and steric contacts of the E–F loop, thus confirming the cyclic structure. Our combined EPR and ODNP results are in agreement with recent NMR studies, which show an α -helical segment between residues 170 and 176, but neither resolve its location with respect to the protein surface, nor reveal the interfacial water dynamics present.^[40–42] The timescale for the water dynamics experienced by the E–F loop residues is found to be consistent with a protein segment with one face exposed to the solvent and the other packed against the protein surface, though still accessible to freely diffusing water molecules, unlike a stable hydrophobic core of a protein (see the Supporting Information, Table S3 and discussion). This finding corroborates recent ssNMR results from hydrogen–deuterium exchange experiments, which show that all E–F loop backbone atoms of PR eventually exchange protons with bulk water.^[28] In addition, the general timescale of the water dynamics that we measured (hundreds of ps) is also consistent with simulations of similar transmembrane channels; these simulations find that a slowdown of water contacting protein surfaces.^[43,44]

Some interesting subtleties in the dynamic environment are revealed by ODNP analysis. For example, around the loop residues outside the two-turn α helix, in the region recent solution-state NMR studies have shown to be part of a short β turn (178–180),^[42] the movement of the translationally mobile water molecules is slower compared to the rest of the loop ($k_o/k_{o,\text{bulk}} < 0.4$, Figure 1 b,) than one might expect from their rather mobile EPR linewidths (Figure S4a in the Supporting Information). The more-rapid water dynamics at the loop surface of the α -helical segment may present “softer” water that facilitates protein movements upon activation. In fact, the fastest water dynamics on the helix are found at the residues that flank the interface between the E–F loop and the protein trunk (A174 and N176; Figure 1 c), which have $k_o/k_{o,\text{bulk}}$ of greater than 0.6 (Figure 1 b), in which case freely diffusing water molecules could be lubricating contact with the protein surface, facilitating photoactivation.

Next, we map out changes in dynamics during conformational motion upon photoactivation by spectroscopically “filming” a slowed photocycle mutant of PR (E108Q) upon

photoactivation with a 532 nm green laser. The E108Q mutation enables the build up of the M photointermediate upon illumination at basic pH (pH 9.5) by slowing the timescale of its decay from milliseconds to seconds.^[45] The M state is thought to involve the largest scale protein movements by analogy to BR.^[35,46–48] Time-resolved EPR was performed by fixing the magnetic field to an EPR frequency of interest (e.g. the center line or an immobile component) and then observing the spectral amplitude as a function of time upon photoactivation (Figure 2). These residue-specific EPR time courses indicate that the decay of M is biexponential, resulting in two timescales, for example, 0.5–1 s and 2–7 s, similar to those found by the detection of global protein motion by time-resolved optical absorption spectroscopy (Figure S5c in the Supporting Information).

Each of the spin-labeled E–F loop residues 171–178 that we confirmed to be part of an α helix, experienced a change in its local environment that translated into a spectroscopically measurable difference, such as an altered rigidity of the spin label or a change in local polarity (Figure 2). The EPR

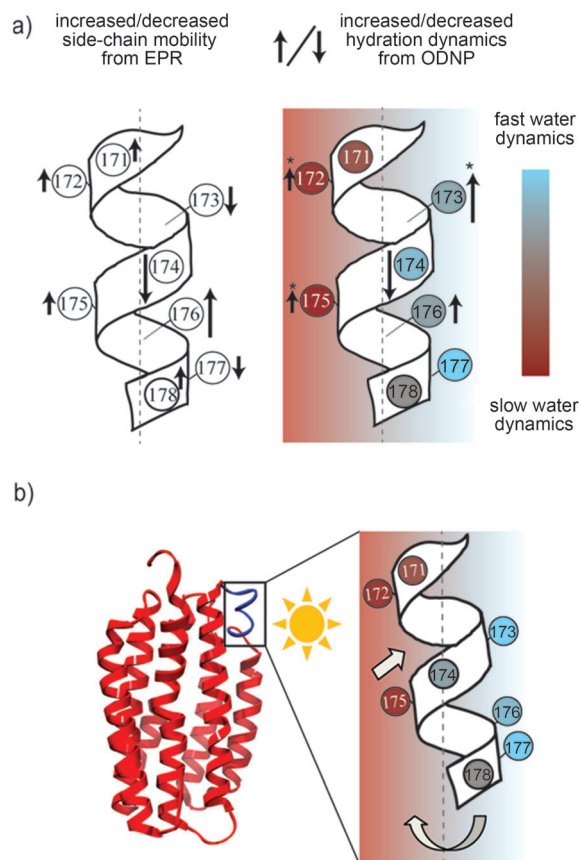


Figure 2. a) Summary of qualitative changes upon photoactivation found from EPR and ODNP results for spin-labeled PR. Arrows indicate increased or decreased dynamics (from ξ or fast ps relaxivity k_o). The size of the arrow reflects the amplitude of the change and an asterisk (*) indicates a decrease in slow (ns) water dynamics (lower k_{low}) and therefore a release of bound water (see the Supporting Information; Figure S2). b) Schematic representation of the conformational switching of the E–F loop of PR upon photoactivation, with the changes in hydration dynamics (ξ) indicated by color grading. See Figure 1 a for values for hydration dynamics parameter ξ upon photoactivation.

linewidths (i.e. spin-labeled protein-segment mobility) are mostly preserved upon photoactivation, suggesting that the E–F loop of PR moves upward and twists as a whole rigid body, only giving rise to changes in the tertiary contact between the spin label and the protein or detergent surface. The buried spin-labeled residues (G171, K172, and C175) show small but distinct increases in mobility, corresponding to a slight lifting of those sites during the formation of the M photointermediate. However, the most flexible sites, S173 and T177, display decreases in their mobile spectral components as well as the center-peak amplitude, thus implying a stiffening of the exposed E–F loop face during the photocycle of PR. The cause of this transient and local immobilization upon photoactivation could be the result of either increased backbone rigidity or an increased interaction with another part of the protein or the surrounding surfactant. The interfacial residues A174 and N176 display opposite changes in mobility that correspond to a twisting motion of the entire loop—A174 becomes immobile, whereas site N176 becomes more mobile. These sites also display the most prominent light-induced EPR spectral differences compared to the other E–F loop residues, which could be due to their positions flanking the protein surface and the surrounding environment.

Finally, we observe significant rearrangement of the E–F loop's hydration water upon photoactivation, manifested by distinct changes in hydration dynamics (ξ , k_o , green traces in Figure 1a and b, and k_{low} , Figure S2 in the Supporting Information). We see similar trends to those seen with EPR, such that increased side-chain mobility corresponds to increased water dynamics and vice versa, except for site S173, where the change presents a more complex interaction (Figure 2a). Fast water diffusion measured by k_o and ξ decreases in the vicinity of A174 and increases around N176 (Figure 1a,b, Figure 2), verifying the twisting motion suggested by the EPR-based map. Interestingly, the mobile residue S173 displays increased water dynamics upon photoactivation, as indicated by the ξ value, while simultaneously experiencing decreased side-chain mobility. The new separation of timescales analysis reveals that this increase in ξ is accompanied by a measurable decrease in k_{low} (Figure S2 in the Supporting Information) while k_o remains unchanged (Figure 1b), implying that the increase is due to the release of tightly-bound water molecules upon photoactivation. A similar effect is noted for the buried residues K172 and C175 (Figure S2).

We must note that the population of photoactivated state may not be large enough for the full degree of the altered hydration dynamics of the light-activated state to be detected, and the extent of the water rearrangement is likely even more dramatic than that shown by these measurements. Nevertheless, it is significant that the residues that make up the α -helical portion of the loop, which we can consider to be a mechanical switch, experience a greater change in hydration dynamics upon activation than selected residues in the loop and transmembrane helices (see Figure 1a and b). This finding supports the idea that the rearrangement of surface hydration water may be intimately coupled to the conforma-

tional change of the α -helical segment that accompanies the activation of PR.

The distinct α -helical structure and significant conformational changes that we observe for the E–F loop could explain previous observations in the literature, which indicate that single mutations^[49–51] or anion binding^[52] to the loop residues can alter the photocycle kinetics and light-absorption properties of PR, even though the loop is remote from the photoactive center. In fact, we have observed functional changes in some of the E–F loop mutants, although the key features of photoactivation are preserved and we expect unaltered conformational changes (see the Supporting Information, Figure S6, and discussion). This study suggests that functional conformational changes could be accompanied by distinct modulation of protein and surface water dynamics, where the rearrangement of surface hydration water may facilitate the propagation of water molecules and/or H^+ across the channel to have a function-tuning effect.

In fact, we observe an altered hydration dynamics landscape for PR reconstituted in lipid bilayer vesicles versus detergent micelles. The ps-scale translational diffusion of free hydration water near the E–F loop of PR embedded in 4:1 DPPC/DOPA vesicles is smaller than in DDM micelles (see the Supporting Information, Table S2; $k_o/k_{o,bulk}$ decreases by a factor of 2–5) and is coupled to a similarly prominent decrease in bound-water contributions ($k_{low}/k_{low,bulk}$ decreases by a factor of 2–6). These effects are likely due to the properties of the lipid membrane itself, which, when spin labeled in the absence of PR, demonstrates similar hydration dynamics to the lipid-embedded PR surface ($k_o/k_{o,bulk} = 0.12$, $k_{low}/k_{low,bulk} = 1.0$ versus PR values of $k_o/k_{o,bulk} = 0.1–0.2$ and $k_{low}/k_{low,bulk} = 2–3$; Table S2 in the Supporting Information). Interestingly, the level of hydration of PR surface residues, when embedded in DPPC/DOPA vesicles, approaches that found at the surface of water-solvated globular proteins^[12] (see the Supporting Information, Table S3 and discussion). This finding suggests that specific features of the hydration dynamics landscape at the ps and ns timescale are critical to facilitating protein function for both water-soluble and lipid-embedded membrane proteins.

With such observations, this study has begun to probe the link between hydration dynamics and transmembrane protein function. In this context, we observe a marked speeding up of the photocycle kinetics for PR embedded in DPPC/DOPA lipid membranes compared to DDM micelles (Figure 3). It is plausible that PR function would be optimal in the more native-like lipid environment, and faster conformational dynamics could enable the wild-type protein to generate a more robust proton gradient by allowing for a faster proton turnover rate, as has been proposed for microbial proton pumps.^[53] We concurrently observe a dramatically altered hydration dynamics landscape near the solvent-contacting surface of the E–F loop, in both the resting and activated states (e.g. for S173R1, $k_o/k_{o,bulk} = 0.51 \pm .03$ in DDM and $0.23 \pm .01$ in lipids, whereas $k_{low}/k_{low,bulk} = 9.6 \pm 0.5$ in DDM and 2.4 ± 0.4 in lipids; see Table S3 in the Supporting Information). This leaves us with the question—could the particular hydration properties of the E–F loop surface, which we observe to be modulated by the surfactant, increase the

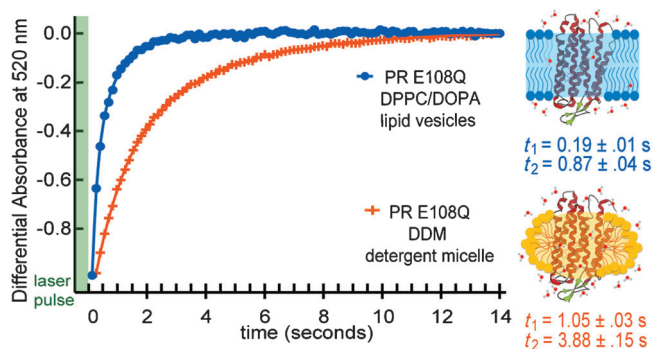


Figure 3. Time-resolved optical absorption spectroscopy to observe the kinetics of M decay at pH 9.5 for PR E108Q embedded either in DDM detergent (red +) or DPPC/DOPA (4:1 w/w) liposomes (blue ●). Characteristic timescales t_1 and t_2 derived from a biexponential fit of the M decay are given. See the Supporting Information for details of data acquisition.

population of water molecules making contact with the channel in such a way as to promote water-mediated proton uptake from the PR surface to its interior? We have introduced an approach that allows the characteristics of transmembrane protein structure and conformational dynamics to interactions to be related with the surrounding hydration water environment at the ps and ns timescales, and can clarify the fundamental and direct role that water may play in tuning membrane protein function.

Received: July 31, 2012

Revised: September 18, 2012

Published online: January 10, 2013

Keywords: dynamic nuclear polarization · EPR spectroscopy · hydration dynamics · membrane proteins · proteorhodopsin

- [1] L. Columbus, W. L. Hubbell, *TRENDS Biochem. Sci.* **2002**, 27, 288.
- [2] D. M. Rosenbaum, S. G. F. Rasmussen, B. K. Kobilka, *Nature* **2009**, 459, 356.
- [3] H. Mchaourab, P. R. Steed, K. Kazmier, *Structure* **2011**, 19, 1549.
- [4] K. Henzler-Wildman, D. Kern, *Nature* **2007**, 450, 964.
- [5] A. McDermott, *Annu. Rev. Biophys.* **2009**, 38, 385.
- [6] L. E. Kay, *J. Magn. Reson.* **2005**, 173, 193.
- [7] B. D. Armstrong, S. Han, *J. Am. Chem. Soc.* **2009**, 131, 4641.
- [8] J. Franck, A. Pavlova, S. Han, *arXiv:1206.0510* **2012**.
- [9] J. H. Ortony, C. Y. Cheng, J. M. Franck, R. Kausik, A. Pavlova, J. Hunt, S. I. Han, *New J. Phys.* **2011**, 13, 015006.
- [10] R. Kausik, S. Han, *Phys. Chem. Chem. Phys.* **2011**, 13, 7732.
- [11] A. Pavlova, E. R. McCarney, D. W. Peterson, F. W. Dahlquist, J. Lew, S. Han, *Phys. Chem. Chem. Phys.* **2009**, 11, 6833.
- [12] B. D. Armstrong, J. Choi, C. López, D. A. Wesener, W. Hubbell, S. Cavagnero, S. Han, *J. Am. Chem. Soc.* **2011**, 133, 5987.
- [13] D. Filmore, *Modern Drug Discovery* **2004**, 24.
- [14] M. Plato, H.-J. Steinhoff, C. Wegener, J. T. TÄ-Rring, A. Savitsky, K. MÄ-Bius, *Mol. Phys.* **2002**, 100, 3711.
- [15] R. Carmieli, N. Papo, H. Zimmermann, A. Potapov, Y. Shai, D. Goldfarb, *Biophys. J.* **2006**, 90, 492.
- [16] C. Altenbach, S. L. Flitsch, H. G. Khorana, W. L. Hubbell, *Biochemistry* **1989**, 28, 7806.
- [17] A. Doll, E. Bordignon, B. Joseph, R. Tschaggelar, G. Jeschke, *J. Magn. Reson.* **2012**, 222, 34.
- [18] H. Frauenfelder, P. W. Fenimore, B. H. McMahon, *Biophys. Chem.* **2002**, 98, 35.
- [19] H. Frauenfelder, G. Chen, J. Berendzen, P. W. Fenimore, H. n. Jansson, B. H. McMahon, I. R. Stroe, J. Swenson, R. D. Young, *Proc. Natl. Acad. Sci. USA* **2009**, 106, 5129.
- [20] K. Mazur, I. A. Heisler, S. R. Meech, *J. Phys. Chem. A* **2012**, 116, 2678.
- [21] D. J. Tobias, N. Sengupta, M. Tarek, *Faraday Discuss.* **2009**, 141, 99.
- [22] K. Wood, M. Plazanet, F. Gabel, B. Kessler, D. Oesterheld, D. J. Tobias, G. Zaccai, M. Weik, *Proc. Natl. Acad. Sci. USA* **2007**, 104, 18049.
- [23] D. C. Mitchell, B. J. Litman, *Biochemistry* **1999**, 38, 7617.
- [24] A. Grossfield, M. C. Pitman, S. E. Feller, O. Soubias, K. Gawrisch, *J. Mol. Biol.* **2008**, 381, 478.
- [25] H. Luecke, *Biochim. Biophys. Acta Bioenerg.* **2000**, 1460, 133.
- [26] N. A. Dencher, H. J. Sass, G. Büldt, *Biochim. Biophys. Acta Bioenerg.* **2000**, 1460, 192.
- [27] J. Yang, L. Aslimovska, C. Glaubitz, *J. Am. Chem. Soc.* **2011**, 133, 4874.
- [28] M. E. Ward, L. Shi, E. Lake, S. Krishnamurthy, H. Hutchins, L. S. Brown, V. Ladizhansky, *J. Am. Chem. Soc.* **2011**, 133, 17434.
- [29] L.-P. Hwang, J. H. Freed, *J. Chem. Phys.* **1975**, 63, 4017.
- [30] M. Bennati, I. Tkach, M. T. Turke in *Electron Paramagnetic Resonance*, Vol. 22, The Royal Society of Chemistry, London, **2011**, p. 155.
- [31] C.-Y. Cheng, J.-Y. Wang, R. Kausik, K. Y. C. Lee, S. Han, *J. Magn. Reson.* **2012**, 215, 115.
- [32] C.-Y. Cheng, J.-Y. Wang, R. Kausik, K. Y. C. Lee, S. Han, *Biomacromolecules* **2012**, 13, 2624.
- [33] M. Pfeiffer, T. Rink, K. Gerwert, D. Oesterheld, H. J. Steinhoff, *J. Mol. Biol.* **1999**, 287, 163.
- [34] U. Alexiev, I. Rimke, T. Pöhlmann, *J. Mol. Biol.* **2003**, 328, 705.
- [35] L. S. Brown, R. Needleman, J. K. Lanyi, *J. Mol. Biol.* **2002**, 317, 471.
- [36] C. Altenbach, K. Yang, D. L. Farrens, Z. T. Farahbakhsh, H. G. Khorana, W. L. Hubbell, *Biochemistry* **1996**, 35, 12470.
- [37] H. Luecke, B. Schobert, H.-T. Richter, J.-P. Cartailler, J. K. Lanyi, *Science* **1999**, 286, 255.
- [38] J. P. Klare, E. Bordignon, M. Engelhard, H. J. Steinhoff, *Photochem. Photobiol. Sci.* **2004**, 3, 543.
- [39] K. Palczewski, T. Kumasaka, T. Hori, C. A. Behnke, H. Motoshima, B. A. Fox, I. Le Trong, D. C. Teller, T. Okada, R. E. Stenkamp, M. Yamamoto, M. Miyano, *Science* **2000**, 289, 739.
- [40] L. Shi, M. A. M. Ahmed, W. Zhang, G. Whited, L. S. Brown, V. Ladizhansky, *J. Mol. Biol.* **2009**, 386, 1078.
- [41] L. Shi, E. M. R. Lake, M. A. M. Ahmed, L. S. Brown, V. Ladizhansky, *Biochim. Biophys. Acta Biomembr.* **2009**, 1788, 2563.
- [42] S. Reckel, D. Gottstein, J. Stehle, F. Löhr, M.-K. Verhoeven, M. Takeda, R. Silvers, M. Kainosho, C. Glaubitz, J. Wachtveitl, F. Bernhard, H. Schwalbe, P. Güntert, V. Dötsch, *Angew. Chem.* **2011**, 123, 12148; *Angew. Chem. Int. Ed.* **2011**, 50, 11942.
- [43] R. J. Law, D. P. Tieleman, M. S. Sansom, *Biophys. J.* **2003**, 84, 14.
- [44] M. S. P. Sansom, I. H. Shrivastava, K. M. Ranatunga, G. R. Smith, *TRENDS Biochem. Sci.* **2000**, 25, 368.
- [45] A. K. Dioumaev, L. S. Brown, J. Shih, E. N. Spudich, J. L. Spudich, J. K. Lanyi, *Biochemistry* **2002**, 41, 5348.
- [46] T. Hirai, S. Subramaniam, J. K. Lanyi, *Curr. Opin. Struct. Biol.* **2009**, 19, 433.
- [47] W. Kühlbrandt, *Nature* **2000**, 406, 569.
- [48] J. Herzfeld, J. C. Lansing, *Annu. Rev. Biophys. Biomol. Struct.* **2002**, 31, 73.

- [49] M. Yoshitsugu, J. Yamada, H. Kandori, *Biochemistry* **2009**, *48*, 4324.
- [50] K. Yamada, A. Kawanabe, H. Kandori, *Biochemistry* **2010**, *49*, 2416.
- [51] S. Y. Kim, S. A. Waschuk, L. S. Brown, K.-H. Jung, *Biochim. Biophys. Acta Bioenerg.* **2008**, *1777*, 504.
- [52] Y. Sharaabi, V. Brumfeld, M. Sheves, *Biochemistry* **2010**, *49*, 4457.
- [53] O. A. Sineshchekov, J. L. Spudich, *Photochem. Photobiol. Sci.* **2004**, *3*, 548.
-